JOURNAL OF SPACECRAFT AND ROCKETS
Vol. 39, No. 6, November–December 2002

Plume Study of a 1.35-kW SPT-100 Using an ExB Probe

Sang-Wook Kim* and Alec D. Gallimore†
University of Michigan, Ann Arbor, Michigan 48109-2118

The ion energy distributions of Xe^{1+}, Xe^{2+}, and Xe^{3+} ions in the SPT-100 plume obtained 50 cm and 1 m from the thruster exit with an ExB probe are presented. Most of the ion species distribution functions exhibit features associated with both Maxwellian and Druyvesteyn distributions. Therefore, the nature of the ion energy distribution in the SPT-100 plume is established by the competing effects of ion acceleration in the discharge chamber and collisional processes beyond the ion production zone. Comparison of beam energy and ion energy spread 50 cm and 1 m from the thruster exit reveal that the energy distribution of the far-field plume ions varies little as the ions move away from the thruster. The angular profiles of the ion species fractions and the beam energy data suggest that, whereas Xe^{2+} and Xe^{3+} ions are produced near the thruster exit, Xe^{1+} ions are created farther upstream in the discharge chamber.

Nomenclature

B	=	magnetic field strength
B	=	magnetic field
E	=	electric field strength
E	=	electric field
E_b	=	ion beam energy
E_i	=	ion energy
e	=	elementary charge; base of natural logarithms
$\boldsymbol{F}$	=	force vector
$f(E_i)$	=	ion energy distribution function
$f(u_i)$	=	ion speed distribution function
$f(\boldsymbol{u}_i)$	=	ion velocity distribution function
I_i	=	channel electron multiplier collector current
q_i	=	charge state of ion
u_b	=	ion beam speed
$\boldsymbol{u}_b$	=	ion beam velocity
u_i	=	ion speed
$\boldsymbol{u}_i$	=	ion velocity
V_f	=	floating potential
V_i	=	acceleration voltage
V_P	=	probe voltage with respect to ground

Introduction

THE closed-drift Hall thruster developed in the former Soviet Union has been under intensive investigation in the United States for the past several years. Because of their efficient use of propellant in producing thrust, Hall thrusters such as the stationary plasma thruster (SPT) can significantly enhance a variety of commercial, scientific, and military space missions by increasing mission life and/or payload mass and by reducing initial spacecraft mass. The high efficiency and high specific impulse of SPTs at low-to-moderate power levels make these devices particularly attractive for north–south stationkeeping.

Past research has shown that the SPT plume consists of multiply charged ions.[1] Production of multiply charged ions in the thruster discharge chamber is a loss mechanism for the thrust, efficiency, and mass utilization.[2] Because of its higher energy, a multiply charged ion causes more erosion of the thruster discharge chamber and spacecraft surfaces, for example, solar arrays, than a singly charged ion accelerated through the same potential drop. Characterizing the energy distribution of each ion species in a Hall thruster plume provides correction factors for engine performance; facilitates a more accurate assessment of thruster discharge chamber erosion, which is directly related to both thruster lifespan and spacecraft contamination; and assists in the successful integration of Hall thrusters with spacecraft. Therefore, it is vitally important to investigate plasma parameters of individual ion species for a complete analysis of the Hall thruster plume. To begin this task, an attempt was made to measure the ion energy distributions of Xe^{1+}, Xe^{2+}, and Xe^{3+} ions in the SPT-100 plume.

The microscopic or kinetic properties of plasma are described by one basic function, the distribution function $f(\boldsymbol{v}, \boldsymbol{r}, t)$. Macroscopic parameters such as density, temperature, and transport properties can all be derived from $f(\boldsymbol{v}, \boldsymbol{r}, t)$ by forming its moments, that is, integrals over velocity space. Then, it is obvious that for a multispecies plasma like the SPT-100 plume, the distribution function of each ion species is needed to characterize the plasma properties fully.

For a steady-state plasma such as the SPT-100 plume, one tries to find $f(\boldsymbol{v})$ or $f(E_i)$ at a certain position in the plasma to derive its macroscopic parameters. In spite of the importance of the ion energy distribution function, there exist only a few techniques for directly measuring $f(E_i)$. The most commonly used device for measuring the ion energy distribution function is the retarding potential analyzer (RPA).[3] However, raw RPA data must be differentiated numerically to obtain the energy distribution, and, thus, any noise in the raw data is magnified when the resulting distribution curves are calculated. Furthermore, the RPA technique can not distinguish different ion species in the thruster plume. A new diagnostic technique developed by King[4] gave species-dependent ion energy distributions by compiling the ion mass spectra for different ion energies. However, this indirect method of obtaining the energy distribution of each ion species resulted in somewhat poor energy resolution.

An ExB probe is a simple diagnostics technique that can separate different ion species according to their velocities. Its use in electric propulsion research has been limited mostly to the investigation of ion thrusters.[2,5–11] In most of these studies, ExB probes were utilized to measure the ratio of doubly charged ions to singly charged ions to provide thrust correction factors and optimum operating conditions for minimum multiply charged ion production.

Because ion thruster plume ions are essentially monoenergetic particles, an ExB probe trace directly gives the ion composition of the plume. In such a case, the ion species fraction is calculated directly from the peak heights of the collected ion currents of each species. The ions in the SPT plume, on the other hand, are produced at different positions in the discharge chamber and, thus, experience

Presented as Paper 99-2423 at the 34th Joint Propulsion Conference, Los Angeles, CA, 20–24 June 1999; received 24 July 2000; revision received 1 May 2002; accepted for publication 27 June 2002.

*Graduate Student, Plasmadynamics and Electric Propulsion Laboratory, Department of Aerospace Engineering; currently Senior Engineer, Advanced Technology Institute, Ltd., 13-1-3 Maeda4jou, Teine-ku, Sapporo, Hokkaido 006-0814, Japan. Member AIAA.

†Associate Professor and Laboratory Director, Plasmadynamics and Electric Propulsion Laboratory, Department of Aerospace Engineering. Associate Fellow AIAA.

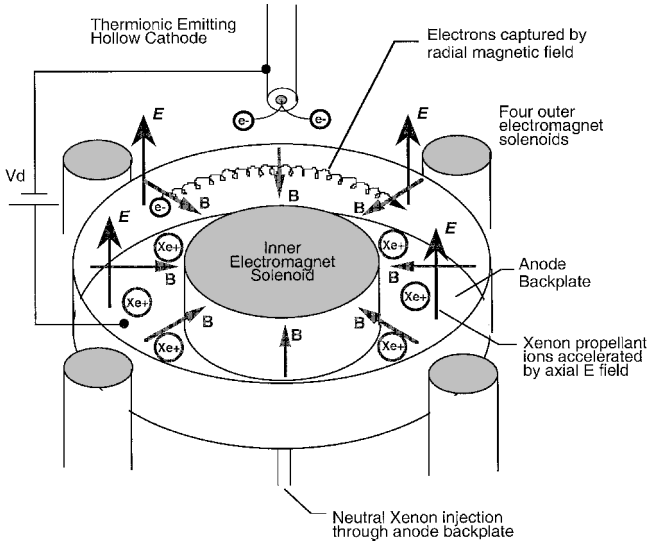

Fig. 1 Schematic of an SPT.

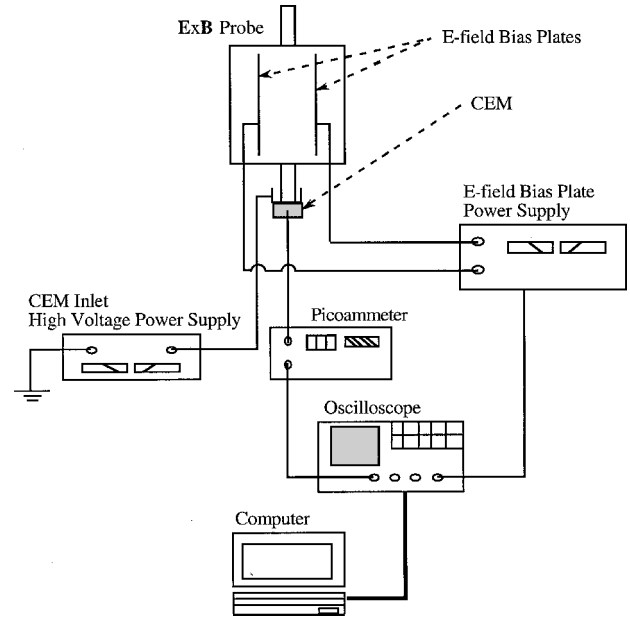

Fig. 2 Schematic of the ExB probe circuit.

different acceleration voltages. Therefore, an ExB probe trace from an SPT plume will have considerably more structure, which must be accounted for in the data analysis. By converting ion velocities into their associated energies, ExB probe data can be used to determine the ion energy distributions in the thruster plume. The study reported here is the first attempt to use an ExB probe to obtain the ion energy distributions in a Hall thruster plume.

Experimental Apparatus

The SPT (Fig. 1) is a coaxial device in which a magnetic field that is produced by an electromagnet is channeled between an inner ferromagnetic core and an outer ferromagnetic ring. This configuration results in an essentially radial magnetic field with a peak strength near the discharge chamber exit of a few hundred gauss. This field strength is such that only the electrons are magnetized. In addition, applying a voltage between the anode and the downstream cathode provides an axial electric field. As the electrons stream upstream from the cathode to the anode, the applied electric and magnetic fields cause them to drift in the azimuthal direction, forming a Hall current. Through collisions, these electrons ionize propellant molecules that are injected through the anode. These ions are then accelerated by the axial electric field and provide the thrust. The mixture of electrons and ions in the acceleration zone means that the plasma is electrically neutral, and, therefore, is not space-charge limited in ion current density. Because the magnetic field suppresses the axial mobility of the electrons while exerting essentially no influence on ion motion, the plasma can support an axial electric field with a potential difference close to the applied voltage between the electrodes. Thus, the bulk of the ions are accelerated through a potential drop that corresponds to approximately 80% of the applied discharge voltage.[4]

The SPT studied in this work is the Fakel SPT-100. For this investigation, the SPT-100 was operated on xenon at its nominal discharge voltage and current of 300 V and 4.5 A, respectively. The anode propellant flow rate was 5.22 mg/s, and the hollow cathode flow rate was 0.28 mg/s. The typical cathode-to-ground potential was −20 V. Before measurements were taken, the thruster was allowed to run for approximately 30 min to reach thermal equilibrium. The SPT-100 operation was stable over the measurement period.

Experiments were conducted in a 9-m-long by 6-m-diam stainless-steel vacuum chamber. During the thruster operation, the background pressure was 1.2×10^{-4} torr (indicated). The ion energy distribution was measured at various angles off thruster axis at a constant axial distance from the thruster center. The thruster was mounted on a rotary table of a multiaxis positioning system. The thruster was mounted in such a way that the rotational axis of the rotary table coincided with the center of the thruster exit plane. The ExB probe was mounted on a stable, fixed platform in front of the positioning system and aligned with the center of the thruster exit plane. With this arrangement, the thruster plume was sampled as a function of angular position at a fixed axial distance from the center of the thruster exit plane by rotating the thruster relative to the fixed probe. The 0-deg position corresponds to the thruster axis, whereas positive angles represent the probe data in the cathode side of the thruster plume. The cathode was in the measurement plane.

The angular measurements were taken at the axial distances of 1 m and 50 cm from the center of the thruster exit plane by moving the thruster and rotary table axially with the axial translation stage. Although the positioning system has an absolute accuracy of 0.15 mm in the axial and 0.1 deg in the rotational directions, initial alignment of the probe with a reference point was only accurate to within 5 mm in the axial and 3 deg in the rotational directions. Hence, the absolute positions for all data have an uncertainty of 5 mm and 3 deg in the respective directions.

Data from the ExB probe were obtained using the probe circuit illustrated in Fig. 2. The voltages to the two E-field bias plates were supplied using a 600-V power supply. One plate was ramped positive, and the other was ramped to the same voltage magnitude negative with respect to ground so that the potential on the probe center axis is at ground. The channel electron multiplier (CEM) was used for the ion detector. The CEM inlet potential, which controlled the multiplier gain, was supplied by a high-voltage power supply. The current signal from the CEM was measured using a picoammeter, which converted the current signal to a voltage signal. The picoammeter voltage signal and the two voltage signals from the E-field bias plates were sent to a digital oscilloscope and then exported to a computer for analysis.

The probe body was kept at the floating potential to minimize the disturbance in the local plume plasma. To account for ions gaining energy as they fell from ambient plasma potential to ground potential on the center axis of the probe, the plasma potential with respect to ground was measured separately with a Langmuir probe. The Langmuir probe mapped the entire region of the plume interrogated by the ExB probe.[4] The entire platform supporting the ExB probe was covered with low-sputter-yield flexible graphite sheets to minimize sputtering due to high-energy ion impact.

A preliminary examination of the probe data showed that the noise-to-signal ratio increased with increasing CEM inlet voltage, that is, increasing gain. This result is counterintuitive because an increase in CEM gain should increase the overall signal-to-noise ratio. The cause of what was observed may be attributed to the onset of CEM saturation by the excessive beam current. Thus, for each measurement, the lowest gain of the CEM that provided a readily measurable output current was selected. Probe measurements were taken five times at each position and averaged to give the final probe trace.

Energy Distribution Function Model

An ExB probe, also known as a Wien filter, is a velocity filter that allows only those ions with the speed $u_i = E/B$ to travel undeflected through the ExB section.[12,13] Because ions with different charge states experience similar accelerating voltages in the discharge chamber of the thruster, the speed of the ions will be a function of their charge state. Hence, the ExB probe can distinguish ions with different charge states. The resolution of the ExB probe used in this study is conservatively estimated to be 1% of the measured ion energy.[14] The probe is calibrated using the ion energy data in Ref. 4. The calibrated value of the magnetic flux density of the ExB probe agrees to within 0.6% of the measured average flux density.[14] The total uncertainty in the ion energy distribution measurements is estimated to be ±2% for the ion current and ±4% for the ion energy. The relation between the ion energy distribution function and the ExB probe trace (after the abscissa of the probe I-V characteristic is converted to ion energy) is

$$f(E_1) \propto I_i(E_i) \Big/ E_i^{\frac{1}{2}} \tag{1}$$

where $I_i(E_i)$ is the probe collector current at the ion energy E_i. Hence, the ExB probe trace represents a true ion energy distribution function.

The ion energy distribution function in the SPT-100 plume plasma has often been assumed to be a Maxwellian in the past. A Maxwellian distribution represents a gas in equilibrium that is achieved by collisions between gas particles. However, the steady-state $f(E_i)$ of the plume ions can not be attributed entirely to collisional processes in the thruster plume. Instead, $f(E_i)$ in the thruster plume is expected to depend strongly on the acceleration voltages V_i. The width of $f(E_i)$ would then depend on the spread in V_i as beam ions are accelerated through in the thruster discharge chamber, as well as collisional processes in the plume.

Another well-known distribution function is the Druyvesteyn distribution. Distributions of this nature are associated with a significant fraction of the particle populations having their energies close to the average energy.[15] Because the ions in the SPT-100 plume would retain the energies that they acquired through the uniform electric field in the thruster discharge chamber, one could imagine that the ions in the thruster plume can be considered as if they were under the influence of a uniform steady electric field. However, the other condition for the Druyvesteyn distribution to be valid, namely, the condition that the ions and neutral atoms must collide elastically, are not met for the ions in the SPT-100 plume where the ion–neutral mean-free-paths are several meters.[14]

From the preceding discussions, the ion distribution function in the SPT-100 plume is expected to be somewhat similar to both Maxwellian and Druyvesteyn distributions. Hence, an attempt was made to model the ion distribution function as a distribution having the form

$$f(u_i) = K' \cdot u_i^2 \cdot \exp\left[-\beta' \cdot (u_i - u_b)^n\right] \tag{2}$$

where K′ and β' are constants. A Maxwellian distribution corresponds to an n value of 2, whereas a Druyvesteyn distribution corresponds to an n value of 4. This approach has been successful in developing electron energy distribution models from probe data.[16,17] Because u_i is proportional to the square root of E_i, Eq. (2) can be cast in terms of E_i as

$$f(E_i) = K \cdot E_i^{\frac{1}{2}} \cdot \exp\left[-\beta \cdot \left(\sqrt{E_i} - \sqrt{E_b}\right)^n\right] \tag{3}$$

Because $(\sqrt{E_i} - \sqrt{E_b})$ can be either positive or negative, the model produces real number solutions only when n is an integer. Therefore, if the assumption is made that the velocity distribution function $f(u_i)$ is symmetric around u_b, Eq. (3) can be rewritten as

$$f(E_i) = K \cdot E_i^{\frac{1}{2}} \cdot \exp\left[-\beta \cdot \left(\left|\sqrt{E_i} - \sqrt{E_b}\right|\right)^n\right] \tag{4}$$

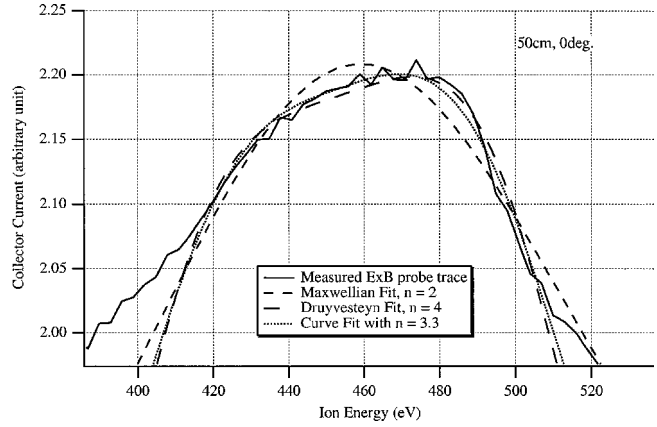

Fig. 3 Comparisons between the Maxwellian fit, Druyvesteyn fit, curve fit of Eq. (5), and the ExB probe trace of Xe^{2+} ion peak, measured on the thruster axis at 50 cm from the thruster exit.

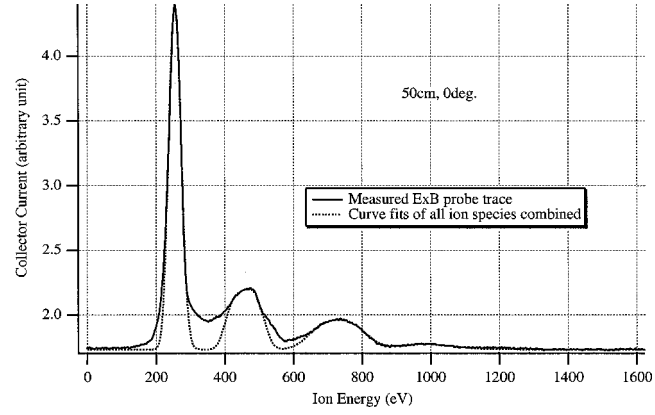

Fig. 4 Sum of the curve fits of Eq. (5) for Xe^{1+}, Xe^{2+}, Xe^{3+}, and Xe^{4+} ion peaks overlaid on the ExB probe trace, measured on the thruster axis at 50 cm from the thruster exit.

When Eq. (4) is combined with Eq. (1), the ExB probe traces can be modeled with

$$I_i(E_i) = K_0 + K_1 \cdot E_i \cdot \exp\left[-\beta \cdot \left(\left|\sqrt{E_i} - \sqrt{E_b}\right|\right)^n\right] \tag{5}$$

where K_0, K_1, β, E_b, and n are fitting parameters. Each peak of the ExB probe traces is then curve fit to Eq. (5) by computer using a Levenberg–Marquardt algorithm that searches for the best fitting parameters.[14,15]

Figure 3 shows a typical fit of Eq. (5) to experimental data. As Fig. 3 shows, the fitting algorithm produced a curve with an n value of 3.3, which agreed very well with the measured probe trace. Notice that this n value lies between 2 and 4, the values for a Maxwellian and Druyvesteyn distribution, respectively. Figure 3 also shows that the model deviates from the measured data at low and high energy ranges. This disagreement between the model and the measured data further from the peaks can be seen more clearly in Fig. 4, which shows the measured probe trace and the sum of the fitted curves for Xe^{1+}, Xe^{2+}, Xe^{3+}, and possibly Xe^{4+} ions. The comparison of the experimental data and their curve fit shows exceptional agreement in the upper part of the peaks. However, the curve fits do not agree with the experimental data at low energy (~200 eV) and in the regions between the peaks. The disagreement at low energy ($E_i < 220$ eV) may be due to significant ion production near the exit plane of the thruster, which results in low-energy ions. The disagreement at low energy may also be due to charge exchange collisions with neutral atoms. The disagreement in the regions between the peaks can be attributed to elastic collisions between the particles of the two ion species that the peaks represent.[4] For example, the overlapped region between the first peak (Xe^{1+} ions) and the second peak (Xe^{2+} ions) is the result of elastic collisions between Xe^{1+} ions and Xe^{2+} ions. The fitted curves can then be thought of as representing the "precollision"

ion distributions. As such, the peak height of the fitted curve must be lower than the true precollision distribution function because the population of ions that have undergone elastic collisions shifts toward the region between the peaks. Incorporating a scheme for predicting elastic collisions would improve the model. However, it is evident from the excellent agreement shown in the upper part of the peaks that this simple model can produce precollision distribution functions very well.

Results and Discussion

Energy distribution functions $f(E_i)$ were obtained by fitting each peak of the ExB probe trace to Eq. (5). From the fitting parameters, E_b and n (the exponential factor) were found for each ion species at various locations in the SPT-100 plume. The spread of ion energy was calculated from the width of the distribution functions. Finally, estimates of ion species fractions were made by forming the first moments of the distribution functions. The errors in the reported data were calculated from the errors in the fitting parameters in the curve fits, which were estimated as the standard deviation for each of the fitting parameters by the computer.

As can be seen from Eq. (5), the value of n indicates how much the distribution is Maxwellian-like or Druyvesteyn-like, where $n = 2$ corresponds to a Mawellian distribution and $n = 4$ corresponds to a Druyvesteyn distribution. Figures 5 and 6 show the variations of n value with respect to angle off thruster axis 50 cm and 1 m from the thruster exit, respectively. Figures 5 and 6 show that most of the ion species distribution functions were somewhere between a Maxwellian and a Druyvesteyn distribution, as expected. Therefore, the energy distribution functions of the beam ions are established by both ion acceleration in the discharge chamber and collisional processes beyond the ion production zone. The former (i.e., the influence of the uniform steady electric field) drives the ions toward a Druyvesteyn distribution, whereas the latter drives the ions toward a Maxwellian distribution.

Figures 5 and 6 also suggest that the distribution functions for Xe^{1+} ions are closer to Maxwellian than those for the ions of higher charge states. This is not surprising because a Maxwellian distribution represents a group of particles in equilibrium where the equilibrium state is achieved by collisions among the particles. Because the ion–ion elastic collision frequency increases with increasing number density,[17] and because the ion beam of the SPT-100 is composed mostly of Xe^{1+} ions,[1,4] these ions are expected to undergo more elastic collisions as a group than higher charge state xenon ions do.

Figures 7 and 8 show the beam energy per charge, E_b/q, of the various ion species at 50 cm and 1 m from the thruster exit, respectively. The beam energy E_b was one of the fitting parameters and represents the most probable energy of the ion species. Bishaev and Kim[18] used a langmuir probe to measure a number of plasma properties inside the discharge chamber of an SPT. According to their measurements, the electron temperature in the discharge chamber attains its maximum value in the region of highest magnetic field strength, which occurs near the thruster exit. Accordingly, because the ionization potential increases with the degree of ionization, it is expected that the formation of multiply charged ions occurs farther downstream in the discharge chamber than where Xe^{1+} ions are produced. Moreover, some of the multiply charged ions are expected to be produced from electron impact ionization of lower charge state ions because the average impact energy required for multistep ionization is lower than that for direct ionization from neutral atoms. Thus, the multiply charged ions would, again, be formed farther downstream than the Xe^{1+} ions. As a result, multiply charged ions should experience less acceleration voltage and have smaller beam energies per charge.

The results in Figs. 7 and 8 show that E_b/q for Xe^{1+} ions is almost always the highest, which supports the ionization and acceleration mechanism discussed earlier. However, E_b/q for Xe^{2+} ions is almost always lower than that of Xe^{3+} ions, which contradicts the ionization mechanism discussed earlier. Hence, the formation of multiply charged ions must be much more complicated than the simple mechanisms discussed. Regardless, the relative closeness of

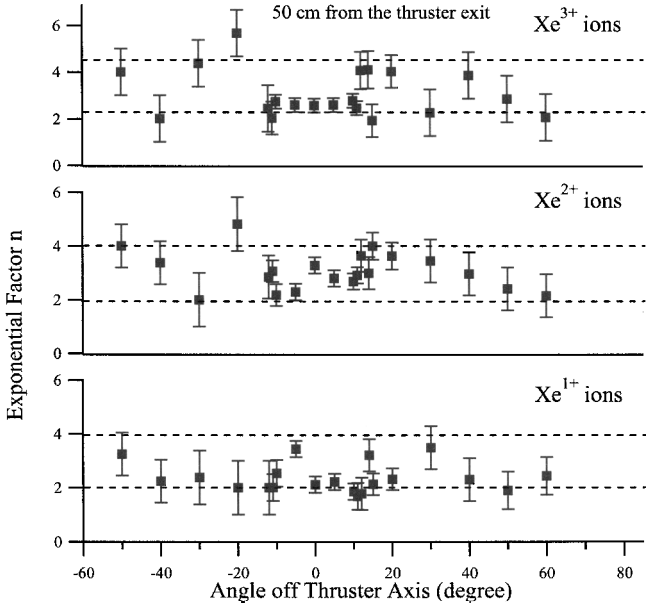

Fig. 5 Exponential factor n in Eq. (5) obtained from the curve fits of the ExB probe data at 50 cm from the thruster exit.

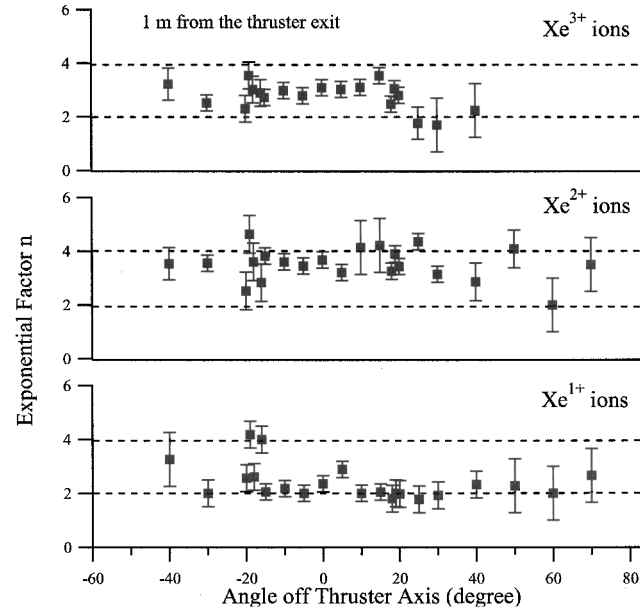

Fig. 6 Exponential factor n in Eq. (5) obtained from the curve fits of the ExB probe data at 1 m from the thruster exit.

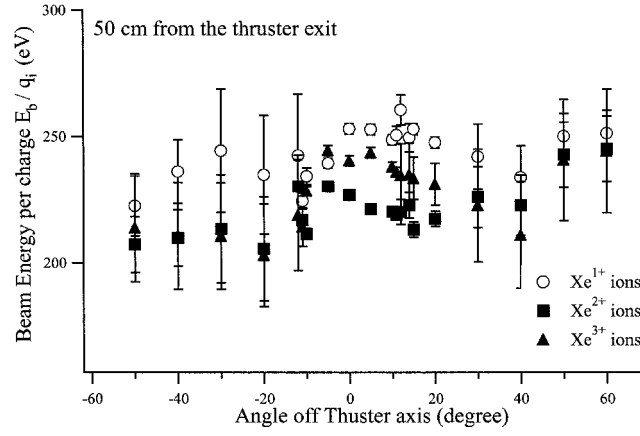

Fig. 7 Beam energy per charge of Xe^{1+}, Xe^{2+}, and Xe^{3+} ions obtained from the curve fits of the ExB probe data at 50 cm from the thruster exit.

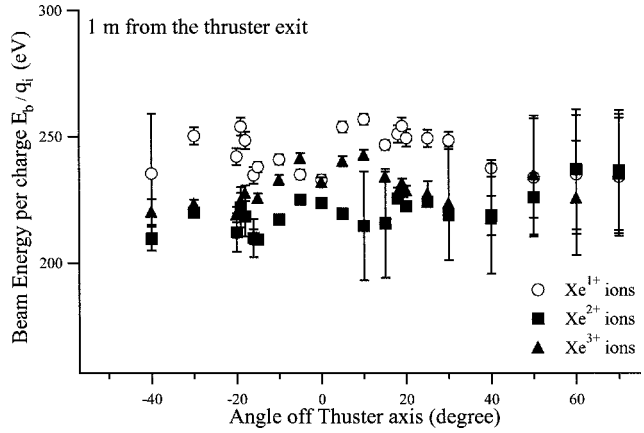

Fig. 8 Beam energy per charge of Xe^{1+}, Xe^{2+}, and Xe^{3+} ions obtained from the curve fits of the ExB probe data at 1 m from the thruster exit.

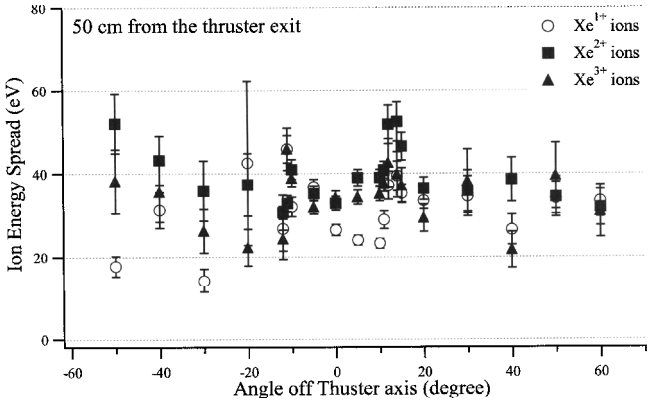

Fig. 9 Spread of ion energy of Xe^{1+}, Xe^{2+}, and Xe^{3+} ions at 50 cm from the thruster exit.

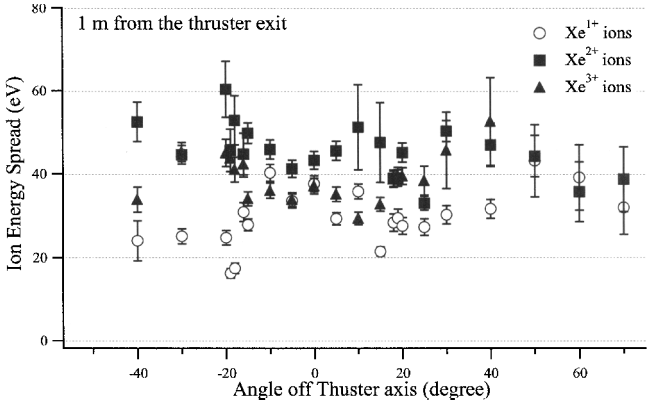

Fig. 10 Spread of ion energy of Xe^{1+}, Xe^{2+}, and Xe^{3+} ions at 1 m from the thruster exit.

the data presented suggests that the three charge state ions are all created within a narrow zone in the SPT discharge chamber.

The spread of ion energy is calculated from the distribution functions as the half-width of $f(E_i)$ at the point where $f(E_i)$ has a value of e^{-1} times the peak value (where $E_i = E_b$ at the peak). In this study, the half-width on the side of the peak where $E_i > E_b$ is used simply because the curve fits have better agreement with the experimental probe trace on that side. Figures 9 and 10 show the results of the energy spread calculations at 50 cm and 1 m from the thruster exit, respectively. The energy spread varies from 20 to 60 eV depending on the angle off thruster axis and the ion species. However, the energy spread is approximately 38 eV within 20 deg off thruster axis. This range of energy spread agrees with the study by King,[4] where he found energy spreads of approximately 20 to 40 eV for the main discharge ion beam.

Table 1 Comparison between raw and corrected ExB probe-measured ion species fractions with values obtained by King[4]

Ion species	Raw ExB probe data	Corrected ExB probe data	Data by King[4]
Xe^{1+}	0.790	0.930	0.888
Xe^{2+}	0.161	0.064	0.110
Xe^{3+}	0.049	0.006	0.002

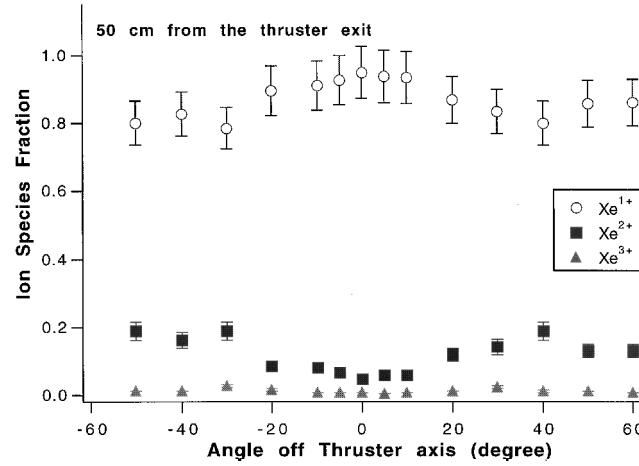

Fig. 11 Ion species fractions of Xe^{1+}, Xe^{2+}, and Xe^{3+} ions at 50 cm from the thruster exit.

Ion species fractions are calculated at each data point by determining the first moment of the distribution functions for each ion species, that is, number density n_i, and calculating the fractions of n_i at the data point. Although a number of ExB probe traces contained peaks that may be associated with Xe^{4+} ions (Fig. 4), the fraction of these high-energy ions is thought to be too low for analysis. Furthermore, these high-energy ion peaks may be the result of background nitrogen and oxygen neutrals that are ingested by the thruster, ionized, and accelerated by the discharge chamber potential drop.[14] Thus, the plume ions are assumed to consist of Xe^{1+}, Xe^{2+}, and Xe^{3+} ions.

The ion species fractions at 5 deg off thruster axis at 50 cm from the thruster exit are compared with the similar data obtained by King[4] (Table 1). The disagreement between the two data sets is attributed to the underestimation of the Xe^{1+} ion fraction in the ExB probe traces due to the curve-fit limitations discussed before and exhibited in Fig. 4. The discrepancy can also be caused by the overestimation of Xe^{2+} and Xe^{3+} ion fractions. Recall that a CEM, a particle detector that exploits secondary electron emission, is used to collect ions for the ExB probe. Because secondary emission yield depends on the energy and charge state of the incident particles,[19,20] a number of multiply charged ions will result in higher output current than the same number of singly charged ions. An estimate of the variation of the secondary emission yield suggests that the output current of Xe^{2+} ions and Xe^{3+} ions are 3 and 10 times larger, respectively, than that of the same number of Xe^{1+} ions.[19,20] If the variation in CEM output due to ion charge state is factored in, the ion species fractions becomes 0.930 for Xe^{1+} ions, 0.064 for Xe^{2+} ions, and 0.006 for Xe^{3+} ions. (See "Corrected" column in Table 1.) Thus, the variation of the secondary emission yield may have overpredicted the multiply charged ion fractions in the raw ExB data.

Figures 11 and 12 show the ion species fractions from corrected ExB data at 50 cm and 1 m from the thruster exit, respectively. The angular profiles of ion species fractions exhibit a sudden change near ±20 deg off thruster axis at both 50 cm and 1 m from the thruster exit. Although the majority of ions in the thruster plume are always Xe^{1+} ions, the fraction of Xe^{2+} ions increases significantly outside of this region. An ion can exit the thruster only if it does not hit a wall before leaving the discharge chamber. Therefore, for an ion to exit the thruster, the ion velocity vector angle with respect to the thruster axis must decrease the farther upstream in the discharge chamber the region of ion production is. Then, the angular profiles of the ion species fractions in Figs. 11 and 12 imply that the Xe^{2+}

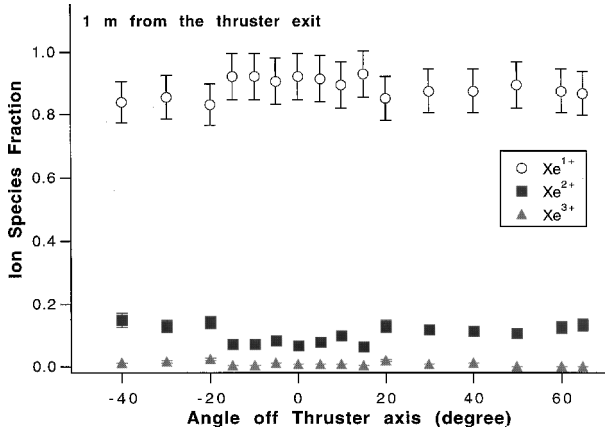

Fig. 12 Ion species fractions of Xe^{1+}, Xe^{2+}, and Xe^{3+} ions at 1 m from the thruster exit.

ions and Xe^{3+} ions are produced closer to the thruster exit than are Xe^{1+} ions. In other words, the region of primary production for Xe^{1+} ions is separated from the primary production region of Xe^{2+} and Xe^{3+} ions by a narrow boundary in the discharge chamber. If one assumes that the ion trajectories are straight lines, this boundary would be located where the line of sight from this region to the exit of the outer discharge chamber wall forms, approximately 10 to 20 deg with respect to the thruster axis. If one assumes further that the primary ion production occurs near the inner wall of the discharge chamber as a previous study suggests,[18] then the primary production of multiply charged ions occurs too far upstream in the discharge chamber (almost at the anode) to account for the angular profiles shown in Figs. 11 and 12. Therefore, the factor limiting the angle of ion velocities may be more than just the discharge chamber geometry for the case of straight-line ion trajectories. Another angle-limiting factor is the influence of the electric field in the discharge chamber on the ions, which makes the ion trajectories more parabolalike rather than straight. Parabolalike trajectories would result if the initial radial velocity component of an ion remains constant while the axial component increases continuously in the axial electric field. Therefore, the actual angle off thruster axis with which the ions can emerge from the discharge chamber is smaller than that of the ions with straight-line trajectories.[14] Thus, both the discharge chamber geometry and the accelerating force of the electric field limit the angle of ions exiting the thruster.

Conclusions

The ion energy distribution $f(E_i)$ of each ion species in the SPT-100 plume is obtained at various angles off thruster axis at 1 m and 50 cm from the thruster exit using an ExB probe. The probe data show that the energy distributions functions of an SPT-100 plume ion is a blend of Maxwellian and Druyvesteyn distributions, suggesting that both ion creation and acceleration in the discharge chamber, and collisional processes beyond the ion production zone, come into play in establishing the ion energy distributions in the plume. The comparison of beam energy E_b and ion energy spread 1 m and 50 cm from the thruster exit reveals that the energy distribution of the plume ions varies little as the ions move away from the thruster in the far field of the thruster plume. The sharp change in the ion species fractions near ± 20 deg off thruster axis, as well as the beam energy data, imply that Xe^{2+} and Xe^{3+} ions are produced closer to the thruster exit than Xe^{1+} ions are. From the ion species fractions data and a simple geometric calculation, it is found that both the discharge chamber geometry and the accelerating force of the electric field limit the angle of ion velocities exiting the thruster.

Acknowledgments

This work was supported by the Air Force Office of Scientific Research, with Mitat Birkan monitoring Grant F49620-95-1-0331. We thank Space Systems/Loral for the loan of the SPT-100 and its power processing unit and acknowledge the support of the departmental technical staff in assisting on maintaining the facilities and experiments. The authors thank the students at the Plasmadynamics and Electric Propulsion Laboratory for their valuable input.

References

[1]Manzella, D. H., "Stationary Plasma Thruster Plume Emissions," International Electric Propulsion Conf., IEPC Paper 93-097, Sept. 1993.

[2]Vahrenkamp, R. P., "Measurement of Double Charged Ions in the Beam of a 30 cm Mercury Bombardment Thruster," AIAA Paper 73-1057, Oct. 1973.

[3]Hutchinson, I., *Principles of Plasma Diagnostics*, 1st ed., Cambridge Univ. Press, New York, 1987, pp. 79–84.

[4]King, L. B., "Transport-Property and Mass Spectral Measurements in the Plasma Exhaust Plume of a Hall-Effect Space Propulsion System," Ph.D. Dissertation, Dept. of Aerospace Engineering, Univ. of Michigan, Ann Arbor, MI, Aug. 1998.

[5]Sovey, J. S., "Improved Ion Containment Using a Ring-Cusp Ion Thruster," *Journal of Spacecraft and Rockets*, Vol. 21, No. 5, 1984, pp. 488–495.

[6]Patterson, M. J., "Performance Characteristics of Ring-Cusp Thrusters with Xenon Propellant," AIAA Paper 86-1392, June 1986.

[7]Kuang, Y.-Z., Guo-Qing, X., and Yang, S.-T., "ExB Momentum Analyzer for Broad-Beam Ion Sources," AIAA Paper 87-1081, May 1987.

[8]Takegahara, H., and Kasai, Y., "Beam Characteristics Evaluation of ETS-VI Xenon Ion Thruster," International Electric Propulsion Conf., IEPC Paper 93-235, Sept. 1993.

[9]Pollard, J. E., "Plume Angular, Energy, and Mass Spectral Measurements with the T5 Ion Engine," AIAA Paper 95-2920, July 1995.

[10]Anderson, J. R., and Fitzgerald, D., "Fullerene Propellant Research for Electric Propulsion," AIAA Paper 96-3211, July 1996.

[11]Nakayama, Y., and Takegahara, H., "C_{60} Application to Ion Thruster–Inspection of Ionized and Extracted Particle," International Electric Propulsion Conf., IEPC Paper 97-076, Aug. 1997.

[12]Roboz, J., *Introduction to Mass Spectrometry Instrumentation and Techniques*, 1st ed., Interscience, New York, 1968, pp. 75–93.

[13]White, F. A., *Mass Spectrometry in Science and Technology*, 1st ed., Wiley, New York, 1968, pp. 101–108.

[14]Kim, S.-W., "Experimental Investigations of Plasma Parameters and Species-Dependent Ion Energy Distribution in the Plasma Exhaust Plume of a Hall Thruster," Ph.D. Dissertation, Dept. of Aerospace Engineering, Univ. of Michigan, Ann Arbor, MI, Aug. 1998.

[15]Lieberman, M. A., and Lichtenberg, A. J., *Principles of Plasma Discharges and Materials Processing*, 1st ed., Wiley, New York, 1994, pp. 88–115.

[16]Rundle, H. W., Clark, D. R., and Deckers, J. M., "Electron Energy Distribution Functions in an O_2 Glow Discharge, " *Canadian Journal of Physics*, Vol. 51, No. 1, 1973, pp. 144–148.

[17]Foster, J. E., "An Investigation of the Influence of a Transverse Magnetic Field on the Formation of Large Anode Fall Voltages in Low-Pressure Arcs," Ph.D. Dissertation, Dept. of Applied Physics, Univ. of Michigan, Ann Arbor, MI, Dec. 1996.

[18]Bishaev, A., and Kim, V., "Local Plasma Properties in a Hall-Current Accelerator with an Extended Acceleration Zone," *Soviet Physics—Technical Physics*, Vol. 23, 1978, pp. 1055–1057.

[19]Bruining, H., *Physics and Applications of Secondary Electron Emission*, 1st ed., McGraw–Hill, New York, 1954, pp. 54–68.

[20]Dekker, A. J., *Solid State Physics*, 1st ed., Prentice–Hall, Englewood Cliffs, NJ, 1965, pp. 166–194.

D. L. Cooke
Associate Editor